Bistatic radar case studies from Antarctica and Greenland

Nicholas Holschuh[1], Knut Christianson[2], Sridhar Anandakrishnan[1], Richard Alley[1]
[1]*Department of Geosciences, The Pennsylvania State University, University Park, PA 16801*
[2]*The Courant Institute of Mathematics, New York University, New York, NY 10012*

The Theory:

Traditional radar surveys are performed with a **common offset** configuration; the radar transmitter and receiver antennae are transported over the survey area, separated by a fixed distance. These surveys provide a single value for reflection amplitude at a given subsurface horizon. There are, however, two primary controls on reflection amplitude outside of the system parameters:

1) Dielectric contrast at the reflection horizon
2) Power losses in transmission through the ice

This makes interpreting amplitudes in common offset surveys an underconstrained problem. Many modern studies attempt to make inferences about material properties and configuration in the subsurface using common offset radar surveys, without any independent means of disentangling these seperate contributions to the reflection power. **Common midpoint** (CMP) surveys have the potential to remove the effects of the reflection horizon, isolating the attenuation and absorption for separate analysis. This is done by imaging the same point using multiple ray paths (by stepping incrementally outward from the target - Fig. 1).

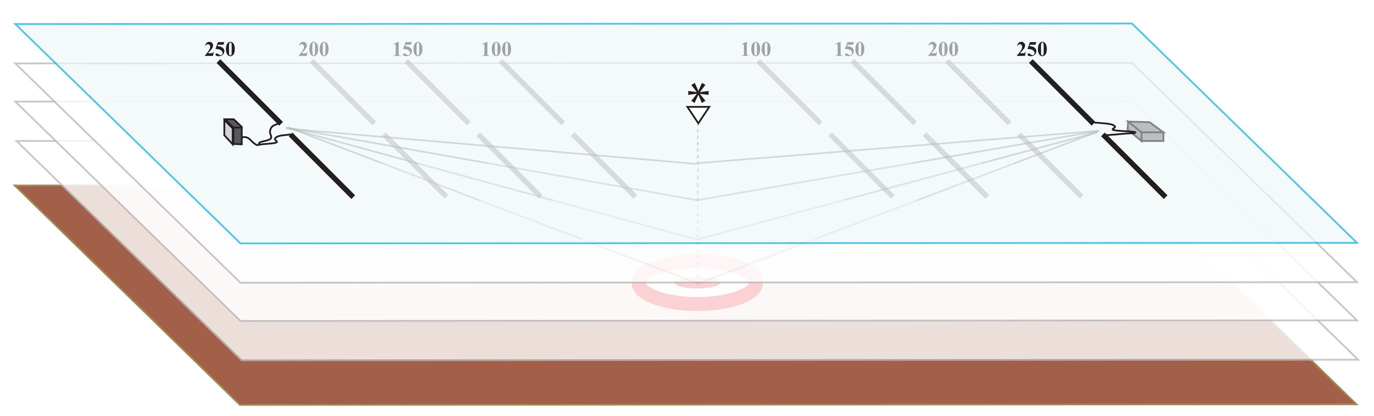

Figure 1. - Schematic of a common midpoint radar survey.

The radar equation highlights the power of radar CMP surveys. Below, we present a modified version of the radar equation as interpreted by Matsuoka et al. (2010), indicating the factors controlling received power ($[P]_{dB}$)

$$[P]_{dB} = [S(\theta,\phi)]_{dB} + [R]_{dB} + [F(\theta)]_{dB} - [L(r)]_{dB} - [G(r)]_{dB} - [B(r,\theta)]_{dB}$$

Some of these parameters are controlled by system configuration and survey geometry. These values can be computed, and corrected for:

$[S(\theta,\phi)]_{dB}$	System directivity	(A function of transmission angle)
$[G(r)]_{dB}$	Power loss from spherical spreading	(A function of ray path-length)
$[F(\theta)]_{dB}$	Power increase from refractive focusing	(A function of transmission angle and path length)

For specular reflectors, the reflectivity is independent of the ray path. As a result, it can be eliminated from the radar equation by examining relative amplitudes collected from the same subsurface location:

$[R]_{dB}$	Interface Reflectivity	(Dielectric contrast between media)

The remaining terms can be computed from the post correction, relative amplitudes:

$[L(r)]_{dB}$	Dielectric Attenuation	(A function of path length and ice properties)
$[B(r,\theta)]_{dB}$	Birefringence	(A function of crystal orientation)

Triggering, Noise, and Sources of Uncertainty

Precise locations and timing are critical to radar CMP analysis. Through differential GPS, we can compute the offsets to sub-centimeter resolution, eliminating almost all uncertainty in the positioning. Synchronizing the radio transmitter with the receiver system is therefore the greatest source of uncertainty resulting from the data collection process.

The method used to synchronize the transmitter and receiver for the presented surveys relies on the air-wave of the imaging radar. At near offsets, there is sufficient power in the direct arrival of the radar wave to trigger the recording device. Using the velocity of EM waves in air, the initiation time for the transmitter can be computed. This system works poorly at far offsets - the amplitude of the air-wave falls within the electrical noise. Lowering the triggering threshold to detect the air-wave results in noise triggered traces. The recorder then spuriously stacks in traces that are not recording any signal. This problem is exacerbated by several factors:

- The radiation pattern for dipole antennae has a transmission node in the plane of the receiver (Fig. 3).
- The receiver system we deploy is powered by a generator, which is a large source of electrical noise.

We have designed an independent RF link, transmitting from an antenna with gain maximized in the direction of the receiver. This set-up works up to several kilometers offset, as long as line of site can be maintained between the two systems.

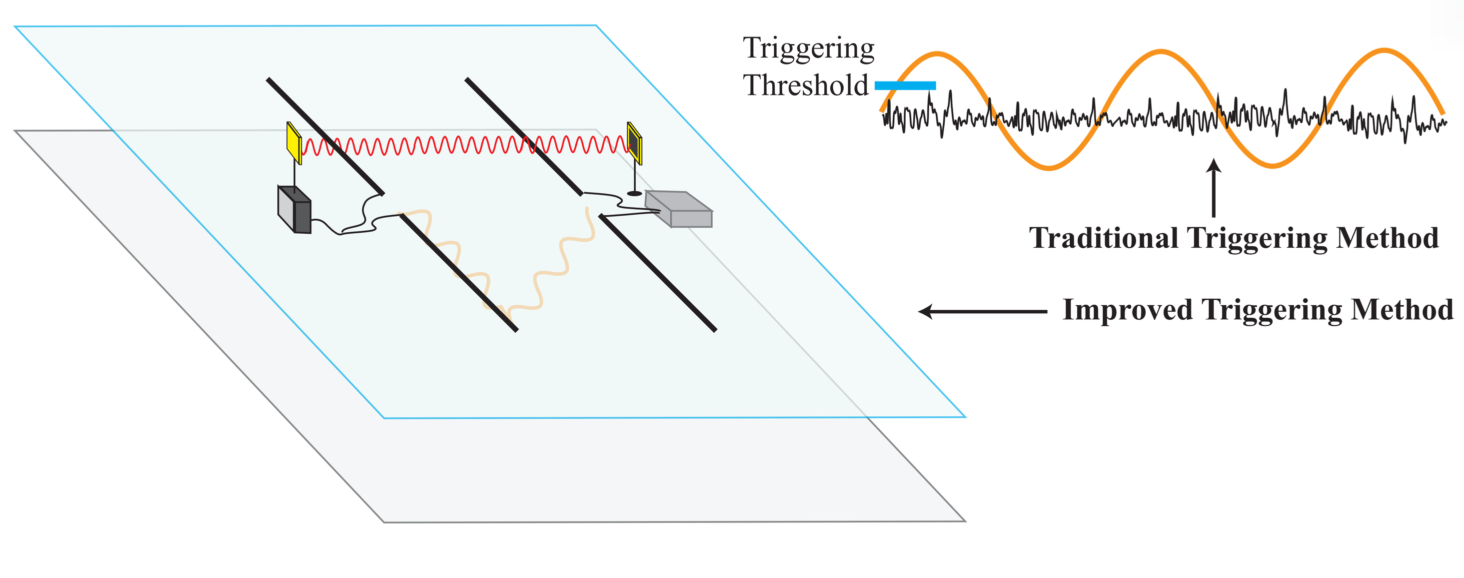

Figure 2. - Schematic of the current triggering method (which uses the imaging radar direction), as well as the improved RF link set-up scheduled for use in the 2014-2015 WAIS divide field season.

Data Processing:

Spherical Spreading

Matsuoka et al. (2010) present a simplified function for the spherical spreading correction for use in common offset surveys:

$$[G]_{dB} = 2\,[\mathrm{h} + z/\sqrt{\varepsilon}\,]_{dB}$$

To accurately compute the spherical spreading correction, we need information about the depth variability of the dielectric constant. This can be approximated by using semblance analysis of the CMP data to determine the EM wave speed as a function of depth.

The wave fronts do not expand as perfect spheres due to refraction in the ice. Therefore, the spherical spreading correction requires a focusing factor. We use a simple two layer model, approximated by the above equation (Bogorodsky et al. 1985).

$$[F]_{dB} = 2\left[\frac{\left(\frac{\mathrm{h}}{z}\right) + 1}{\left(\frac{\mathrm{h}}{z}\right) + \left(\frac{\tan\ \theta_1}{\tan\ \theta_2}\right)}\right]_{dB}$$

Radiation Pattern and Radar Gain

The overall transmitted power of the radar system is consistent from trace to trace, and therefore is irrelevant when looking at relative reflection amplitude. The transmitter and receiver antennae, however, have gain levels that vary as a function of their angle from vertical (θ) and orientation in the horizontal plane (ϕ). The antennae used in the surveys described below were a simple dipole. We performed the radiation correction using the gain functions below (Engheta et al. 1982). Note, the radiation pattern depends on the index of refraction for englacial transmission. We assume a simple two layer model.

for $\theta < \pi/2$

$$S_1(\theta,\phi) = S_0\left\{\left[\frac{\cos^2\theta}{\cos\theta + (n^2 - \sin^2\theta)^{1/2}} - \sin^2\theta\,\cos\theta\frac{\cos\theta - (n^2 - \sin^2\theta)^{1/2}}{n^2\cos\theta + (n^2 - \sin^2\theta)^{1/2}}\right]^2 \cos^2\theta + \frac{\cos^2\theta\,\sin^2\phi}{(\cos\theta + (n^2 - \sin^2\theta)^{1/2})^2}\right\}$$

for $\pi/2 < \theta < \pi - \mathrm{asin}(n^{-1})$

$$S_2(\theta,\phi) = S_0\left\{\left[\sin^2\theta\cos\theta\frac{(1 - n^2\sin^2\theta)^{1/2} + n\cos\theta}{n(1 - n^2\sin^2\theta)^{1/2} - \cos\theta} - \frac{\cos^2\theta}{(1 - n^2\sin^2\theta)^{1/2} - n\cos\theta}\right]^2 + \frac{\cos^2\theta\,\sin^2\phi}{(1 - n^2\sin^2\theta)^{1/2} - n\cos\theta)^2}\right\}$$

for $\pi - \mathrm{asin}(n^{-1}) < \theta < \pi$

$$S_2(\theta,\phi) = S_0\left\{\frac{(n^2 - 1)\sin^4\theta\cos^2\theta\cos^2\phi - 2\cos^2\phi\sin^2\theta\cos^4\theta}{n^2(n^2\sin^2\theta - 1) + \cos^2\theta} - \frac{\cos^4\theta\,\cos^2\phi + \sin^2\phi\cos^2\theta}{(n^2 - 1)}\right\}$$

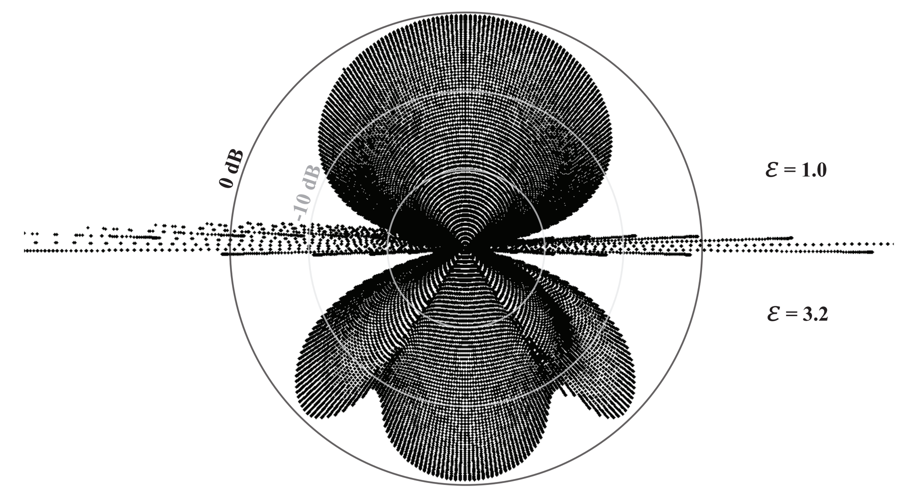

Figure 3.- Computed radiation pattern for a dipole antenna (oriented to best display the E-Plane). These antennae are optimized for imaging at nadir, and therefore gain corrections must be applied to accurately determine the englacial attenuation for non-nadir angles.

Data from Previous Surveys:

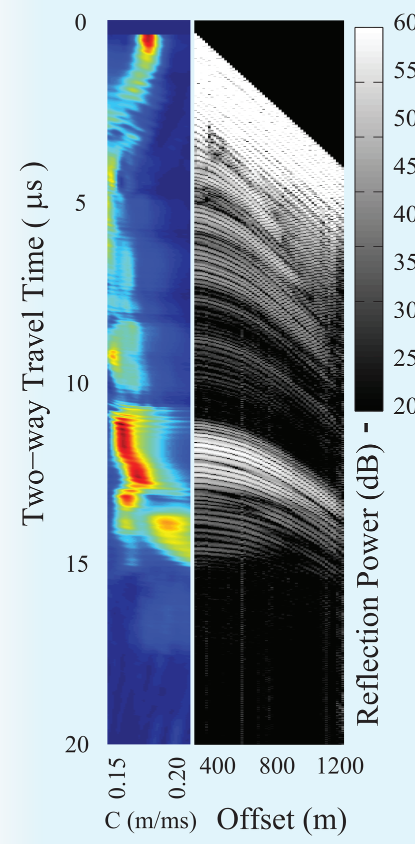

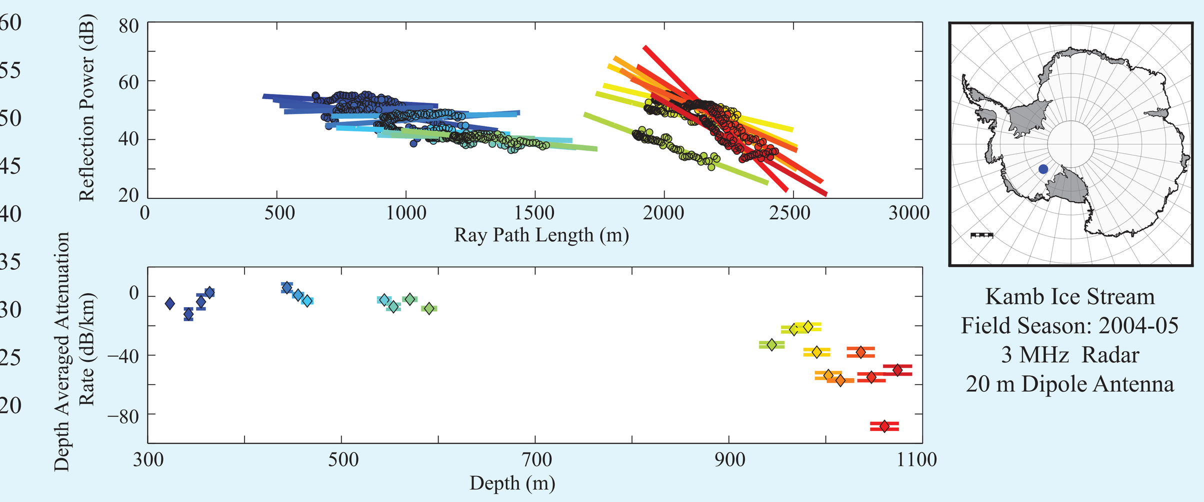

Of the four surveys presented, the Kamb survey yeilded the best results. This is in large part due to the number of traces collected (out to 1200 m maximum offset, with 20 m spacing). Clear internal layers can be traced for analysis, providing a nearly complete depth profile. The horizons stacking in below the bed, which appear to have higher velocities, are likely due to off-axis reflectors. The bed roughness that produces these reflections leads to a complicated attenuation signal in these reflectors.

Conclusion: Roughness at the bed cannot be easily disentangled from the signal.

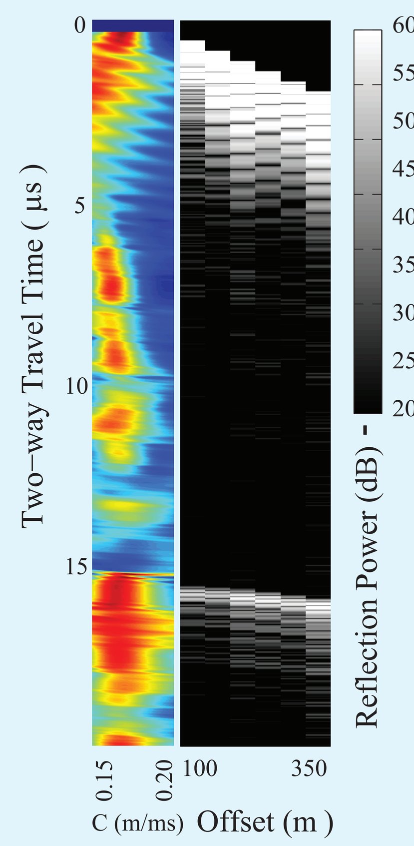

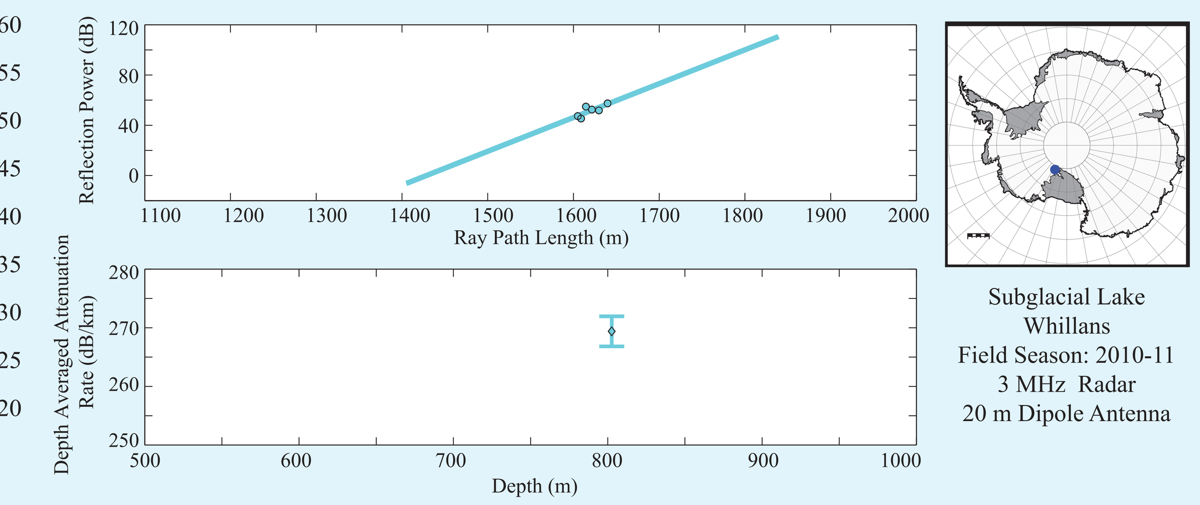

This survey had a very low signal-to-noise ratio. The semblance analysis shows layers stacking in at reasonable velocities in the 5 to 12 μs range, despite no pickable horizons. The collection of additional component traces at each offset would have likely imaged internal reflectors that could have been used in attenuation analysis.

Conclusion: Collecting too few traces at each offset will result in a low signal-to-noise ratio, reducing the usability of results.

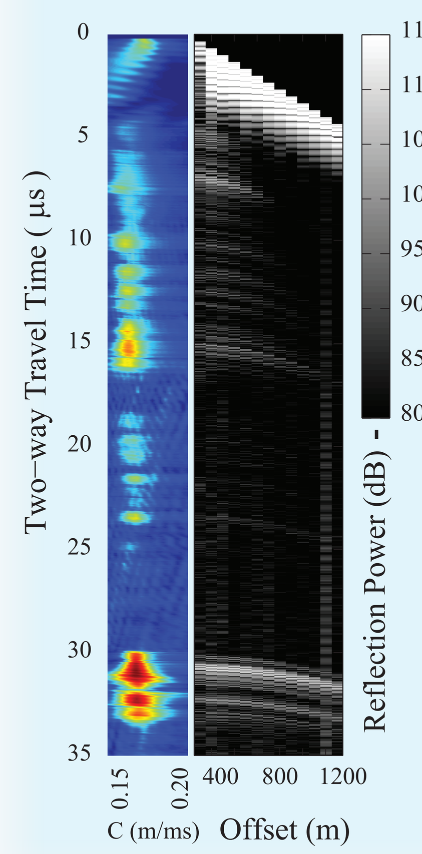

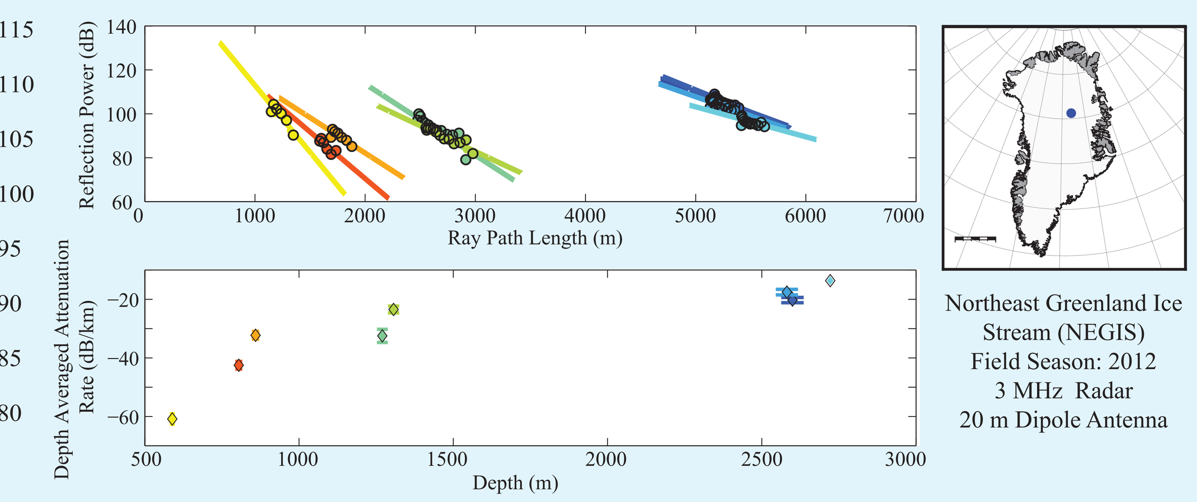

The NEGIS survey shows the second best data quality; however, this survey suffered from significant triggering problems, reducing the overall number of traces stacked into each offset. The common offset profiles collected in this region show 20-30 bright internal layers, that if detected in the CMP could have provided a high resolution record of the attenuation profile with depth. Collecting data with shorter offset spacing could also significantly reduce uncertainty in computed attenuation rates.

Conclusion: Triggering problems result in the collection of spurious traces that can be filtered before stacking, but may result in lower than desired signal-to-noise.

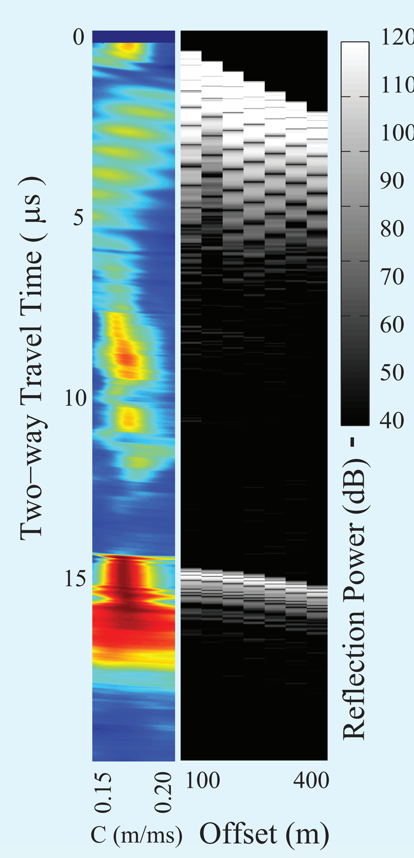

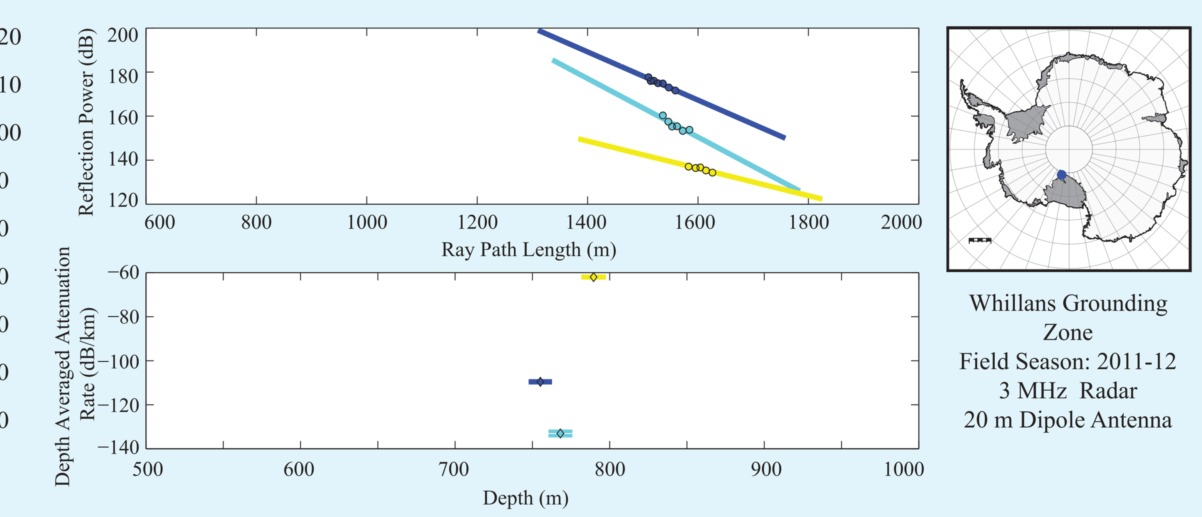

There is a clear basal reflector in this data, however the range of offsets and number of offset samples is too few to get a reliable fit for the attenuation profile. There is an 80 dB/km spread between the three reflectors picked, highlighting the need for larger data sets to reduce uncertainty in regression parameters.

Conclusion: Accurate estimates of attenuation require a wide range of offsets.

WAIS Divide Survey - 2014/15 Season

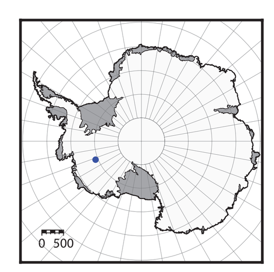

During the upcoming field season, we will be conducting a radar CMP survey at the WAIS divide in West Antarctica. This is an ideal test case for radar CMPs:

1) It is colocated with a complete ice core, which provides direct measurements of the temperature and chemical profile of the ice sheet there (i.e. - controls on attenuation).

2) During the same field season, we will also be conducting a seismic CMP survey. This provides a third method for cross-checking the ice thickness. If the seismic, core, and radar all agree, this survey will provide a proof of concept for colocated radar/seismic CMP surveys in the future.

The ultimate goal of these surveys is to use attenuation profiles to make inferences about ice chemistry and temperature. To determine whether or not this is feasible, further case studies should be performed at the location of current and historic drilling. Ice cores provide the only reliable means of method validation, making WAIS Divide an ideal location for the next radar CMP.

Conclusions

We make the following recommendations for radar CMP survey design:
- The survey should continue to offsets roughly equal to ice thickness
- The offset spacing should be as low as possible (< 50 m)
- The traces should be collected individually, to prevent stacking in noise

Difficult to interpret data resulted primarily from inacurrate triggering and poor spatial sampling.

Acknowledgements

We would like to thank the groups who collected the presented data (UC Santa Cruz and St. Olaf College [Kamb], Pennsylvania State University [NEGIS] and the WISSARD project [Subglacial Lake Whillans and the Whillans grounding zone]). This project is an extension of the work done by Rickard Pettersson, Bob Jacobel, and Joe MacGregor, who presented the preliminary results of the Kamb surveys at the European Geophysical Union annual conference in 2007.

References

Bogorodsky, V., Bentley, C., & Gudmandsen, P. (1985). Radioglaciology (1st ed., p. 254). Dordrecht, Holland: D. Reidel Publishing Co.

Engheta, N., Papas, C., & Elachi, C. (1982). Radiation patterns of interfacial dipole antennas. Radio Science, 17(6), 1557–1566.

Matsuoka, K., Morse, D., & Raymond, C. F. (2010). Estimating englacial radar attenuation using depth profiles of the returned power, central West Antarctica. Journal of Geophysical Research, 115(F2), F02012.